

# Large-scale magnetic field perturbation arising from the 18 May 1980 eruption from Mount St. Helens, Washington

R.J. Mueller and M.J.S. Johnston

*U.S. Geological Survey, Menlo Park, CA 94025 (U.S.A.)*

(Received December 1, 1987; revision accepted March 10, 1988)

Mueller, R.J. and Johnston, M.J.S., 1989. Large-scale magnetic field perturbation arising from the 18 May 1980 eruption from Mount St. Helens, Washington. *Phys. Earth Planet. Inter.*, 57: 23–31.

A traveling magnetic field disturbance generated by the 18 May 1980 eruption of Mount St. Helens at 1532 UT was detected on an 800-km linear array of recording magnetometers installed along the San Andreas fault system in California, from San Francisco to the Salton Sea. Arrival times of the disturbance field, from the most northern of these 24 magnetometers (996 km south of the volcano) to the most southern (1493 km S23° E), are consistent with the generation of a traveling ionospheric disturbance stimulated by the blast pressure wave in the atmosphere. The first arrivals at the north and the south ends of the array occurred at 26 and 48 min, respectively, after the initial eruption. Apparent average wave velocity through the array is  $309 \pm 14 \text{ m s}^{-1}$  but may have approached  $600 \text{ m s}^{-1}$  close to the volcano. The horizontal phase and the group velocity of  $\sim 300 \text{ m s}^{-1}$  at periods of 70–80 min, and the attenuation with distance, strongly suggest that the magnetic field perturbations at distances of 1000–1500 km are caused by gravity mode acoustic-gravity waves propagating at F-region heights in the ionosphere.

## 1. Introduction

At 1532 UT on 18 May 1980, collapse of the north side of Mount St. Helens, Washington, triggered a focused eruption of about  $10^{17}$  J or 24 megatons (Kieffer, 1981) that devastated the region to the north of the volcano. The sudden injection of mass and energy (shock waves) into the atmosphere generated dynamic atmospheric waves that coupled to the ionosphere and were detected at distances as much as 8211 km away by high-frequency Doppler sounder data, Faraday rotation data, microbarograph records (Liu et al., 1982), measurements of the ionospheric total electron content (Roberts et al., 1982) and magnetic observatory data (Fougere and Tsacoyeanes, 1980). At that time the U.S. Geological Survey was operating a linear array of 24 absolute magnetometers along the San Andreas fault system of California in a general northwest–southeast direction (Daul

and Johnston, 1980; Mueller et al., 1980) and a magnetometer on Mount St. Helens. We report here the observations of disturbance arrival times, amplitudes and form through the San Andreas array and four other magnetometers located closer to the volcano. These records suggest that high-frequency electromagnetic disturbances are related to the volcanic eruption.

Other eruptions (Pekeris, 1939), earthquakes (Davies and Baker, 1965; Row, 1966; Yuen et al., 1969; Weaver et al., 1970), nuclear explosions (Hines, 1967; Najita et al., 1975; Simons et al., 1981) and meteors (Whipple, 1930) have excited detectable global atmospheric waves with, in some cases, associated ionospheric disturbances (Row, 1967; Albee and Kanellakos, 1968; Davis, 1973; Roberts et al., 1982; Wolcott et al., 1984). The existence of a linear array of magnetometers along the San Andreas fault allows us to determine the propagation velocity and dispersion characteristics

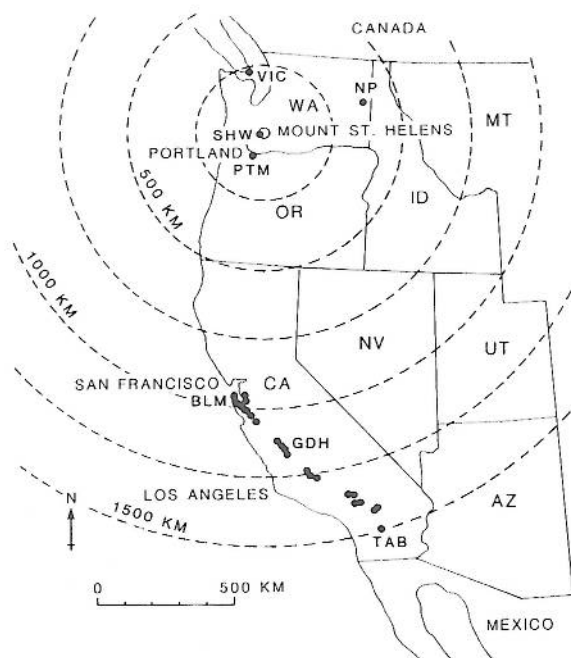


Fig. 1. Location of recording magnetometers at Mount St. Helens (SHW), Portland, Oregon (PTM), Victoria, Canada (VIC), Newport, Washington (NP) and 24 locations along San Andreas fault in California at the time of the 18 May 1980, eruption from Mount St. Helens.

of the disturbance related to the Mount St. Helens eruption.

## 2. Observations

Locations of the recording stations used in this study in relation to Mount St. Helens ( $46.2^{\circ}\text{N}$ ,  $122.2^{\circ}\text{W}$ ) are shown in Fig. 1. All stations record magnetic field intensity at the Earth's surface (Mueller et al., 1980). Magnetometers at VIC, NP and PTM are operated by the Victoria Magnetic Observatory, the U.S. Geological Survey and Carson Helicopter, respectively. One-minute digital data values were recorded at station VIC, and analog records from stations NP and PTM were digitized at 3- and 1-min intervals, respectively. All the other magnetometers were sampled synchronously at 10-min intervals. The total magnetic field data from all the sites during the period 1400–2400 h UT on 18 May 1980, are shown as a

function of great circle distance from Mount St Helens in Fig. 2. Superimposed on the longer-term diurnal signal is an easily identified oscillatory signal that occurs systematically later with increasing distance from the Volcano.

The signals are distinctly different from those of the normal diurnal variation or magnetic storms that generally occur simultaneously across the network of instruments. To illustrate this, Fig. 3 shows simultaneous records of the Mount St. Helens disturbance and examples of typical magnetic field disturbances recorded for a 3-h period on various days across the network. The magnetic observatory at Fredricksburg, Virginia, located at approximately the same magnetic latitude as the California network, recorded quiet magnetic field conditions on 18 May 1980. There is little doubt that the disturbance fields shown in Fig. 2 are a consequence of the eruption of Mount St. Helens.

To isolate the short-term oscillatory signals and to identify their primary characteristics, the longer-term data from each site were fitted with a cubic spline function, and this fit was subtracted from the data. The residual records at each site, after removal of the long-term diurnal variations, are plotted in the same form as in Fig. 2 and are shown in Fig. 4.

The data from either Fig. 2 or Fig. 4 can be used to estimate the apparent horizontal propagation velocity of the disturbance through the magnetometer array. Table I lists the great circle distance of each site from Mount St. Helens, the time of the first change or break (A) (either positive or negative), the subsequent peak (B), the next peak of opposite sense (C), and the amplitude of the first disturbance pulse with respect to the pre-eruption magnetic field level. The period of the first pulse is determined from the difference between the A and C occurrence times.

It is clear from Figs. 2 and 4 that the characteristics of the observed magnetic field perturbations at stations at less than 500 km (near stations) are different from those at more than 1000 km (far stations). As shown in Fig. 5, the near stations indicate that the initial disturbance has a horizontal wave velocity of  $580 \pm 5 \text{ m s}^{-1}$ . The magnetic field perturbations at the near stations have more high-frequency content, and the amplitude of the

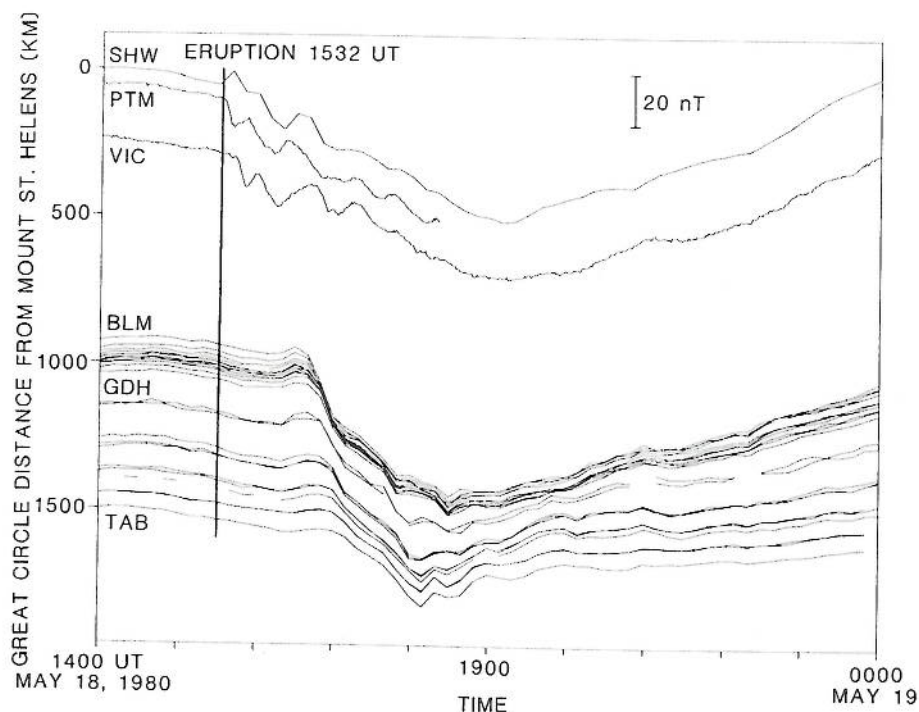


Fig. 2. Time history plots as a function of great circle distance from Mount St. Helens from 1400 to 2400 UT on 18 May 1980. Eruption occurred at 1532 UT. Location of magnetometers is shown in Fig. 1.

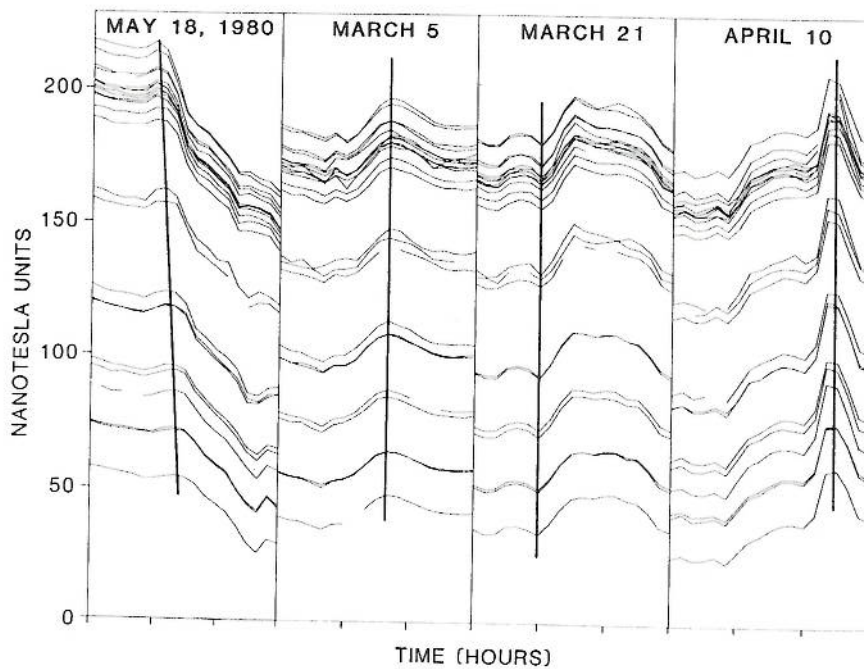


Fig. 3. Examples of magnetic disturbances recorded across the 500 km San Andreas array of instruments on day of eruption and other days of typical disturbed magnetic field. Sloping line drawn through the values, on 18 May, denote differences from normal diurnal variations or magnetic storm responses.

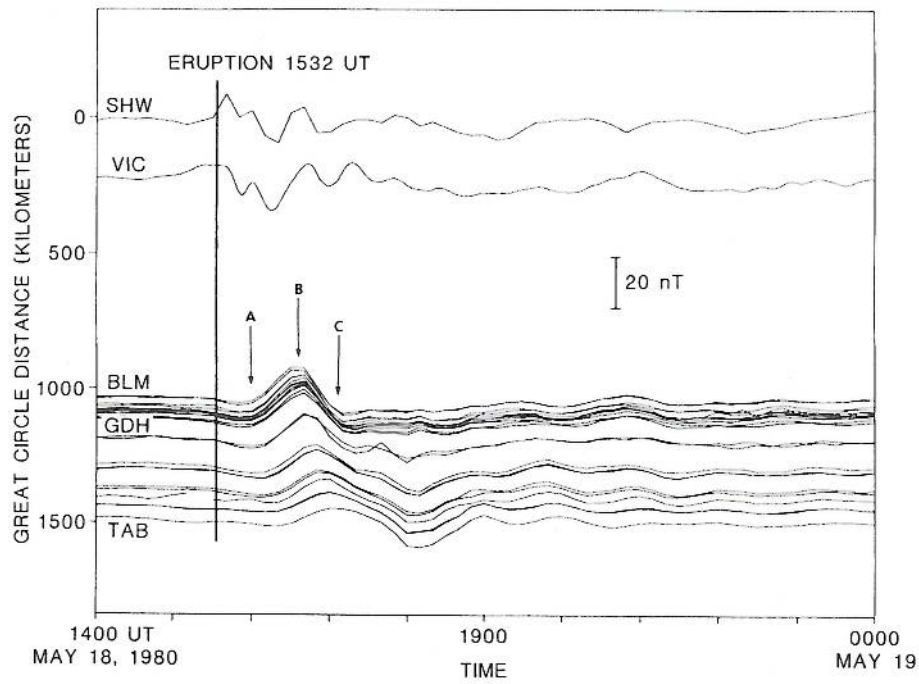


Fig. 4. Residual time history plots as in Fig. 2, with the diurnal variation and other longer-term effects removed by fitting a spline to the long-term data and subtracting this fit from the data.

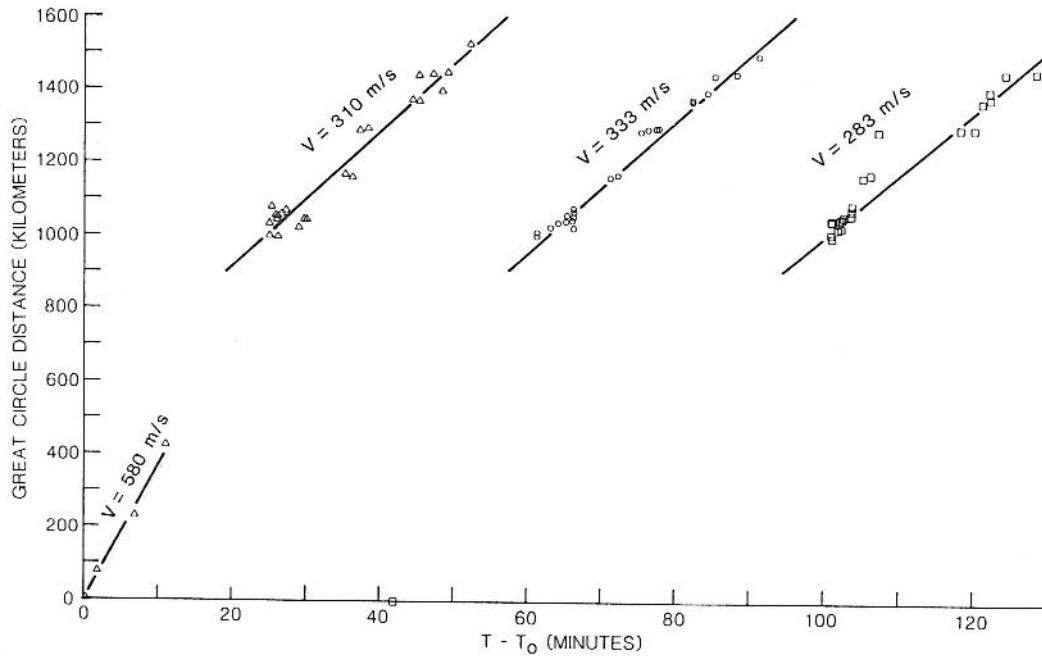


Fig. 5. Plot of disturbance arrival times vs. great circle distance from Mount St. Helens, for each observation point. A linear fit to these data determined the average velocities ( $V$ ).

first pulse varies from 21 to 10 nT. The far stations have horizontal wave velocities that range from  $333 \pm 17$  to  $283 \pm 10$  m s<sup>-1</sup>, with an average of  $309 \pm 14$  m s<sup>-1</sup> (Fig. 5), and longer periods (70–80 min). The amplitude of the first pulse at the far stations decreases from  $\sim 10$  to 5 nT at a rate of  $0.01 \pm 0.001$  nT km<sup>-1</sup> in a linear manner as distance increases from Mount St. Helens (Fig. 6).

Data from the near stations indicate perturbations with periods from 15 to 40 min that cannot be identified in the data sets from the far stations. Interference from these shorter-period waves prevents determinations of wave velocity for other

than the first break (Fig. 5). It should be noted that these data for the near stations were obtained from different observatories, and two of the data sets were digitized from analog records, which lowered the time and magnetic field resolution.

Interaction of the different period waves in the data from the near stations prevents the detection of changes in the period of these perturbations with distance or time. There is a suggestion that the period of the initial disturbance increased from 60 min, at the near stations, to 80 min over the 1500 km distance to the southern stations, but this cannot be derived from these data with certainty. The propagation of the disturbance through

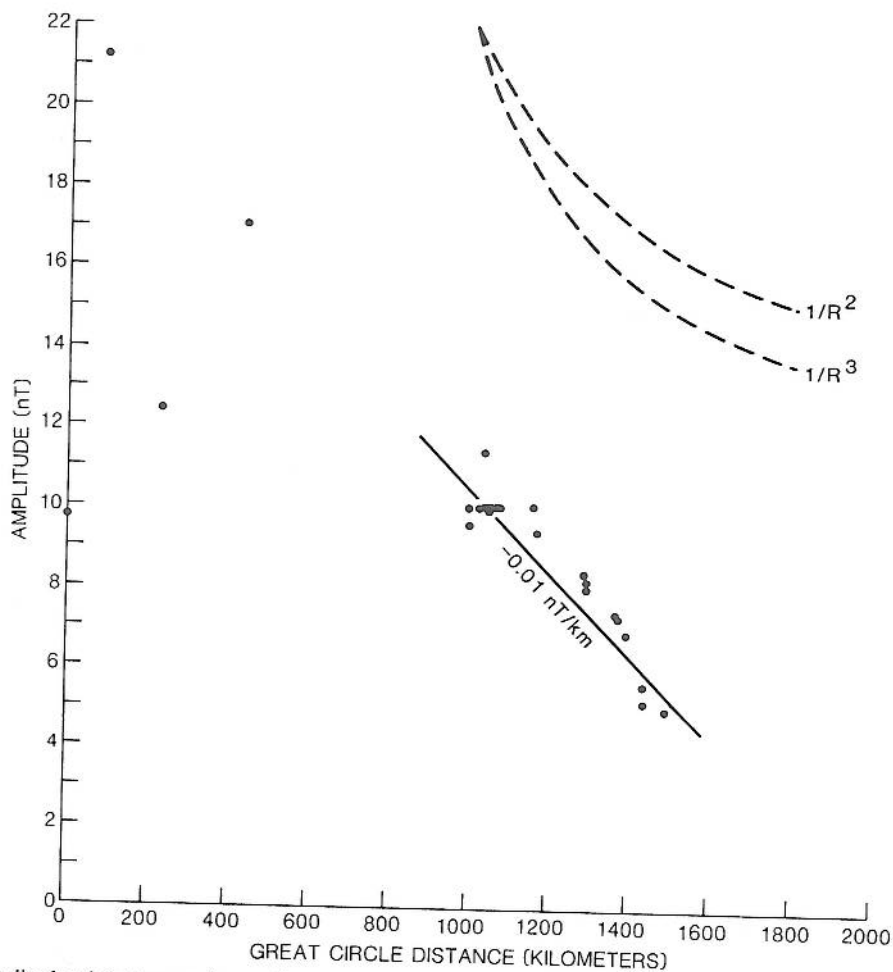


Fig. 6. Plot of amplitude of first anomalous pulse vs. great circle distance from Mount St. Helens. Least-squares fit to data, from stations  $> 900$  km from Mount St. Helens, indicate a linear amplitude decrease of  $0.01 \pm 0.001$  nT km<sup>-1</sup>. Least count sensitivity of these magnetometer stations is 0.25 nT. For comparison, dashed lines indicate form of  $1/R^2$  and  $1/R^3$  attenuation with distance.

TABLE I

Occurrence times of first break (A), subsequent peak (B), next peak of opposite sense (C), and peak-to-peak amplitude between first and second break ( $|B-A|$ ) of the disturbance pulse at each observation point as a function of great circle distance from Mount St. Helens, Washington. Arrows in Fig. 4 indicate location of A, B, and C for data from station BLM. Occurrence times given represent hour and minute on 18 May 1980 in UT.

Site	Great circle distance (km)	Time (A)	Time (B)	Time (C)	Amplitude (nT)
SHW	5	1532	1545	1617	9.7
PTM	80	1534	1602	1625	21.1
VIC	230	1539	1614	1641	12.4
NP	430	1544	1614	1633	17
BLM	996	1558	1635	1713	10.0
MTH	999	1557	1636	1713	9.6
SAR	1034	1557	1636	1713	11.4
EUC	1023	1600	1635	1714	10.1
COY	1022	1600	1638	1713	10.1
ANZ	1042	1602	1638	1714	10.1
NAN	1042	1601	1637	1714	10.1
QSB	1049	1558	1637	1713	10.0
SNJ	1046	1558	1638	1714	9.9
SJN	1050	1558	1638	1714	10.1
LEW	1068	1559	1638	1715	10.0
HAR	1056	1559	1637	1715	10.0
BVL	1079	1557	1638	1715	10.1
LGC	1159	1608	1643	1717	10.0
GDH	1169	1607	1644	1718	9.4
STG	1284	1609	1647	1719	8.4
CHU	1292	1610	1648	1730	8.2
ABL	1292	1610	1649	1732	8.0
PAL	1362	1617	1654	1733	7.4
BUR	1370	1616	1654	1734	7.3
SSK	1391	1620	1656	1734	6.9
LSB	1437	1617	1655	1738	5.6
OCH	1440	1619	1659	1740	5.2
TAB	1493	1620	1703	1747	5.0

the San Andreas array appears to show dispersion with distance from Mount St. Helens, but the data were not sampled rapidly enough for this to be uniquely demonstrated with spectral analysis techniques. The amplitude of the observed disturbance clearly decreases with distance from Mount St. Helens.

### 3. Discussion

The data indicate that a large traveling magnetic field disturbance was generated by the explosive eruption of Mount St. Helens on 18 May 1980. Eruptions, earthquakes, meteors, and nuclear explosions commonly excite global atmospheric waves (Whipple, 1930; Pekeris, 1939; Davies and Baker, 1965; Row, 1966; Hines, 1967; Yuen et al. 1969; Weaver et al., 1970; Najita et al., 1975; Simons et al., 1981), and ionospheric disturbances (Row, 1967; Albee and Kanellakos, 1968; Davis, 1973; Roberts et al., 1982; Wolcott et al., 1984) that result from guided waves in the atmosphere. Guided waves of this sort and associated traveling ionospheric disturbances (Row, 1967; Yeh and Lui, 1974; Francis, 1975) are probably the physical cause of these magnetic field data.

Two basic kinds of models are used to study guided acoustic-gravity waves propagating through the Earth's atmosphere:

(1) free wave propagation through an isothermal atmosphere where boundaries and discontinuities are ignored, and

(2) guided wave propagation where boundaries and discontinuities are important. As we know, the Earth's atmosphere is not isothermal; temperature varies as a function of height, and the application of models based on guided waves probably better approximates the real properties found in the atmosphere. We should state here that, in reality, both approaches are likely to be involved in the process, which results in atmospheric and ionospheric disturbances. Studies that merge the two approaches do not exist at present.

Francis (1973) has determined the properties of various guided modes for acoustic-gravity waves propagating in a realistic atmosphere. These guided modes are subdivided into three main groups: acoustic, Lamb, and gravity. Their primary characteristics are summarized in Figs. 7 and 8.

The series labeled  $A_i$  represents the acoustic mode. The main features of waves in this mode are higher-frequency oscillations with periods less than the buoyancy frequency or Brunt-Väisälä frequency (Väisälä, 1925; Brunt, 1927), horizontal phase velocities from 300 to 750 m s<sup>-1</sup>, and attenuation distances from 3000 to 100 000 km.

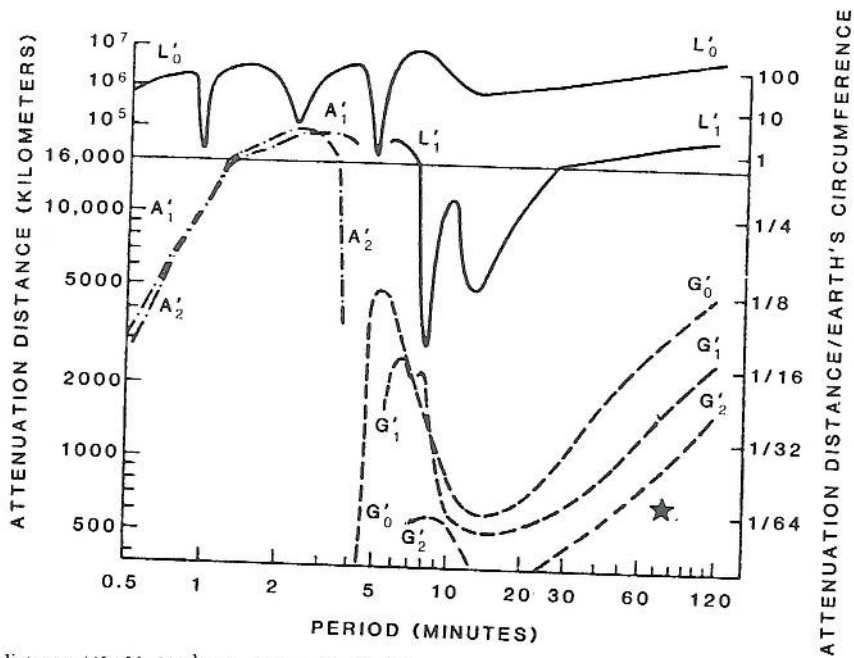


Fig. 7. Attenuation distance ( $|\text{Im}[k_x]|^{-1}$ ) vs. period ( $2\pi/w$ ) for acoustic-gravity waves in the atmosphere, from Francis (1973).  $|\text{Im}[k_x]|^{-1}$  is the distance a mode can propagate before its amplitude has been attenuated by a factor of  $1/e$ . Curves represent different modes: acoustic ( $A_i$ ), Lamb ( $L_i$ ), and gravity ( $G_i$ ). Star (\*) indicates location of the observed magnetic field disturbance.

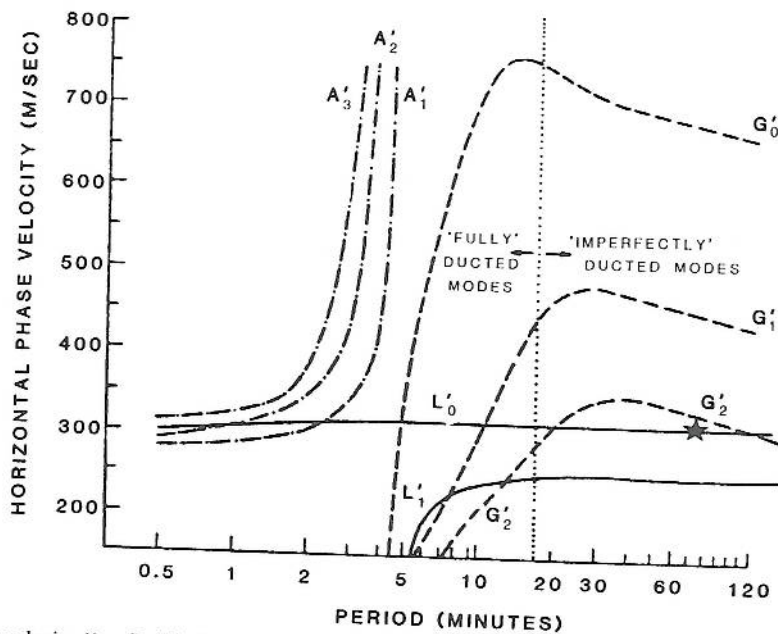


Fig. 8. Horizontal phase velocity ( $(w/\text{Re})[k_x]$ ) vs. period ( $2\pi/w$ ) for acoustic-gravity waves in the atmosphere, from Francis (1973). Curves represent different modes: acoustic ( $A_i$ ), Lamb ( $L_i$ ), and gravity ( $G_i$ ). Star (\*) indicates location of the observed magnetic field disturbance.

Acoustic mode waves travel through the lower atmosphere, at heights below 100 km. Both velocity and attenuation distance are dependent on the oscillatory period of the wave.

The series labeled  $L_i$  represent the Lamb mode. These waves are dependent on the Earth's surface in the ducting process, are nearly nondispersive at all frequencies, and have horizontal phase velocities of 311 or 254 m s<sup>-1</sup>. The Lamb mode waves exist only in the lower atmosphere, at heights below 100 km, and travel for great distances (> 3000 km).

The series labeled  $G_i$  represent the gravity mode. These waves are oscillatory and have frequencies greater than the buoyancy frequency and horizontal phase velocities, ranging from 300 to 750 m s<sup>-1</sup>. The velocities are frequency dependent, and waves of this mode exist in the upper atmosphere between 100 and 500 km; most of the energy is at heights of ~ 300 km (Francis, 1973). For oscillatory periods > 15 min, the attenuation distance for the gravity mode increases as the period increases, but the attenuation distance does not exceed 5000 km (Fig. 8).

The traveling disturbances observed in the 18 May 1980 magnetic field data at the far stations have oscillatory periods ranging from 70 to 80 min, velocities of 283–333 m s<sup>-1</sup>, and attenuation (by a factor of 1/e) of ~ 630 km (Figs. 7 and 8). Although not a perfect fit, these characteristics best fit those of a gravity mode (see  $G'_2$  on Figs. 7 and 8). The 18 May magnetic field disturbances observed at the Earth's surface resulted from waves affecting the F region in the ionosphere (at heights > 130 km), and the gravity mode has substantial energy at these heights (Francis, 1973).

The observed disturbance at the near stations indicate a propagation velocity of 580 m s<sup>-1</sup> with an oscillatory period between 15 and 60 min, but the data are complicated by high-frequency waves that are not observed at the far stations. These characteristics would also be consistent with the gravity mode, where oscillation periods between 10 and 30 min have horizontal attenuation distances from 300 to 500 km for  $G'_2$ .

Other acoustic, ionospheric, and magnetic field data on disturbances generated by the Mount St. Helens explosion have been reported (Ritsema,

1980; Fougere and Tsacoyeanes, 1980; Liu et al., 1982; Roberts et al., 1982). While some of these data sets are too small to describe adequately the complex phenomena generated in the atmosphere and ionosphere after the eruption, each set indicates a propagation velocity of ~ 300 m s<sup>-1</sup> for the first disturbance between distances of 1000 and 2000 km, generally consistent with that reported here. Our data, however, uniquely indicate that the practice of assigning a velocity on the basis of disturbance arrival time, after an eruption at one fixed distance, would give results that have little physical meaning. Apparently, coupled-mode generation occurred in the near field of the volcano.

#### 4. Conclusions

After the 18 May 1980 eruption at Mount St. Helens, we observed magnetic field transients on an array of 25 synchronized magnetometers at distances ranging from 5 to 1493 km. The eruption sent a shock wave and heat pulse into the atmosphere which initiated a traveling ionospheric disturbance that propagated to horizontal distances > 1500 km from Mount St. Helens. Between distances of 1000 and 1500 km, the horizontal propagation velocity of the disturbance is well determined at  $309 \pm 14$  m s<sup>-1</sup> with an oscillatory period of 70–80 min. The velocity and period, together with indications of attenuation and disturbance of the magnetosphere, suggest that the primary physical mechanism is the gravity mode of an acoustic-gravity wave. These data are consistent with gravity mode acoustic-gravity waves in the ionosphere-atmosphere (Francis, 1973).

#### Acknowledgements

We thank L. Law and Don Auld for the magnetic data from the Victoria Geomagnetic Observatory, Carson Geoscience Co. for the data recorded at the Portland airport, S. Silverman for his program on least-squares error analysis, and S.H. Francis for the use of Figs. 7 and 8.

## References

- Albee, P.R. and Kanellakos, D.P., 1968. A spatial model of the F-region ionospheric traveling disturbance following a low-altitude nuclear explosion. *J. Geophys. Res.*, 73: 1039–1053.
- Brunt, D., 1927. The period of simple vertical oscillations in the atmosphere. *Q. J. R. Met. Soc.*, 53: 30–31.
- Daul, W.B. and Johnston, M.J.S., 1980. Catalog of locations of U.S.G.S. instruments recording low frequency data in California—1980. U.S. Geol. Sur. Open-File Rep. 80–704.
- Davies, K. and Baker, D.M., 1965. Ionospheric effects observed around the time of the Alaskan earthquake of March 28, 1964. *J. Geophys. Res.*, 70: 2251–2253.
- Davis, M.J., 1973. The integrated ionospheric response to internal atmospheric gravity waves. *J. Atmos. Terr. Phys.*, 35: 929–959.
- Fougere, P.F. and Tsacoyeanes, C.W., 1980. AFGM magnetometer observations of Mount St. Helens eruption. *EOS Trans. Am. Geophys. Union*, 61: 1209–1210.
- Francis, S.H., 1973. Acoustic-gravity modes and large-scale traveling ionospheric disturbances of a realistic, dissipative atmosphere. *J. Geophys. Res.*, 78: 2278–2301.
- Francis, S.H., 1975. Global propagation of atmospheric gravity waves: a review. *J. Atmos. Terr. Phys.*, 37: 1011–1054.
- Hines, C.O., 1967. On the nature of traveling ionospheric disturbances launched by low-altitude nuclear explosions. *J. Geophys. Res.*, 72: 1877.
- Kieffer, S.W., 1981. Blast dynamics at Mt. St. Helens on 18 May 1980. *Nature (London)*, 291: 568–570.
- Liu, C.H., Klostermeyer, J., Yeh, K.C., Jones, T.B., Robinson, T., Holt, O., Leitinger, R., Ogawa, T., Sinno, K., Kato, S., Ogawa, T., Bedard, A.J. and Kersley, L., 1982. Global dynamic response of the atmosphere to the eruption of Mount St. Helens on 18 May 1980. *J. Geophys. Res.*, 87: 6281–6290.
- Mueller, R.J., Johnston, M.J.S. and Keller, V., 1980. U.S. Geological Survey magnetometer network and measurement techniques in western U.S.A. U.S. Geol. Sur. Open-File Rep. 81–1346.
- Najita, K., Huang, Y.N. and Fang, G.T.N., 1975. Ionospheric disturbances detected over Hawaii after the 1969 French thermonuclear explosion. *Ann. Geophys.*, 31: 301–310.
- Pekeris, C.L., 1939. The propagation of a pulse in the atmosphere. *Proc. R. Soc. London A*, 171: 434–449.
- Ritsema, A.R., 1980. Observations of Mount St. Helens eruption. *EOS Trans. Am. Geophys. Union*, 61: 1201–1202.
- Roberts, D.H., Klobuchar, J.A., Fougere, P.F. and Hendrickson, D.H., 1982. A large-amplitude traveling ionospheric disturbance produced by the 18 May 1980 explosion of Mount St. Helens. *J. Geophys. Res.*, 87: 6291–6301.
- Row, R.V., 1966. Evidence of long-period acoustic-gravity waves launched into the F region by the Alaskan earthquake of March 28, 1964. *J. Geophys. Res.*, 71: 343–345.
- Row, R.V., 1967. Acoustic-gravity waves in the upper atmosphere due to a nuclear detonation and an earthquake. *J. Geophys. Res.*, 72: 1599–1610.
- Simons, D.J., Rickel, D.G., Wolcott, J.H., Duncan, L.M., Bernhardt, P.A., Broste, W.B. and Albee, P.R., 1981. The ionospheric response to a 600-ton H.E. experiment at White Sands. *EOS Trans. Am. Geophys. Union*, 62: 979.
- Väisälä, V., 1925. Über die Wirkung der Windschwankungen auf die Pilot Beobachtungen. *Comment. Phys. Math. II*, 19: 37.
- Weaver, P.F., Yuen, P.C., Prolss, G.W. and Furumoto, A.S., 1970. Acoustic coupling into the ionosphere from seismic waves of the earthquake at Kuril Islands on August 1, 1969. *Nature (London)*, 226: 1239–1241.
- Whipple, F.J.W., 1930. The great Siberian meteor and the waves, seismic and aerial, which it produced. *Q. J. R. Met. Soc.*, 56: 278–304.
- Wolcott, J.H., Simons, D.J., Lee, D.D. and Nelson, R.A., 1984. Observations of an ionospheric perturbation arising from the Coalinga earthquake of May 2, 1983. *J. Geophys. Res.*, 89: 6835–6839.
- Yeh, K.C. and Lui, C.H., 1974. Acoustic-gravity waves in the upper atmosphere. *Rev. Geophys. Space Phys.*, 12: 193–216.
- Yuen, P.C., Weaver, P.F., Suzuki, R.K. and Furumoto, A.S., 1969. Continuous traveling coupling between seismic waves and the ionosphere evident in May 1986 Japan earthquake data. *J. Geophys. Res.*, 74: 2256–2264.